Materials Research Proceedings 28 (2023) 1245-1253 https://doi.org/10.21741/9781644902479-135

Machining of PAM green Y-TZP: Influence of build and in-plane directions on cutting forces and surface topography

SPITAELS Laurent[1,a *], RIVIÈRE-LORPHÈVRE Edouard[1,b]
MARTIC Grégory[2,c], JUSTE Enrique[2,d] and DUCOBU François[1,c]

[1] Machine Design and Production Engineering Lab - Research Institute for Science and Material Engineering - University of Mons, Place du Parc 20, Mons, Belgium

[2] Belgian Ceramic Research Centre, Avenue Gouverneur Cornez 4, Mons, Belgium

[a] laurent.spitaels@umons.ac.be, [b] edouard.rivierelorphevre@umons.ac.be, [c] g.martic@bcrc.be, [d] e.juste@bcrc.be, [e] francois.ducobu@umons.ac.be

Keywords: Green Ceramics, Pellet Additive Manufacturing, Milling, Surface Topography, Hybrid Manufacturing

Abstract. The combination of the pellet additive manufacturing (PAM) process and green ceramic machining within the same hybrid machine is a very promising route to obtain green ceramic parts with complex shapes, smooth surface topography and tight tolerances. However, there is still a lack of data due to the novelty of this manufacturing route. This article studies the possible influence of the build and in-plane directions on the cutting forces and surface topography during the milling of Y-TZP green ceramic parts obtained by the PAM process. The RMS cutting forces, arithmetic and total roughness (Ra and Rt, respectively) were measured. The in-plane direction (aligned with one of the horizontal part edges) did not have a significant influence neither on the cutting forces nor on the surface topography. Conversely, the build direction has a significant effect on the cutting forces recorded. The layers deposited the furthest from the build platform required 57.5% less force to be milled than those in contact with it. The surface topography was not significantly modified across the build direction, all values of Ra were within the 0.8 μm Ra class while all Rt values were < 5 μm.

Introduction

Context. Advanced ceramic materials (such as zirconia) are essential for a large set of sectors thanks to their properties (very high melting point and hardness, chemical inertness, *etc.*) [1,2]. However, the conventional manufacturing routes for ceramics are limited to relatively simple designs and require finishing operations (machining, polishing, grinding or lapping) which can represent up to 80% of the total manufacturing costs [2]. Indeed, these operations are usually performed on the fully sintered part which has the final properties of the material.

On the one hand, green ceramic machining has demonstrated its potential to ease the finishing of the part while reducing the costs and risk to generate macro defects as cracks [3,4]. On the other hand, additive manufacturing (AM) processes open new possibilities to generate near net shape parts with complex design while enabling the production of small or unique part in an economical way [5,6].

Material extrusion process, one of the seven AM processes defined in ISO 52900 standard, is feeding great hopes in a ten year horizon [7]. Indeed, it allows the generation of parts made of metal or ceramics at low cost [8]. Moreover, its variant relying on pellets and screw extrusion, Pellet Additive Manufacturing (PAM) can be fed with feedstock developed for the Ceramic Injection Molding (CIM) or Metal Injection Molding (MIM) industry to shape green parts with complex design. Though, the surfaces generated by the PAM process still suffer from the staircase effect and exhibits high arithmetic roughness (Ra ranging from 9 μm to 40 μm) impacting their

fatigue resistance and tribological properties [9-11]. Finishing these parts is then required before foreseeing their usage for demanding applications such as contact (requiring Ra < 1.6 µm, *e.g.*). Nonetheless, even if green ceramic machining can be very attractive thanks to its advantages, it is still limited to simple designs. Lattice, internal surfaces and channels, which can be required in the freeform designs of biomedical implants, are then impossible to finish by machining operations [4,12].

The combination of the green ceramic machining and PAM process inside the same hybrid machine can overcome the disadvantages of both processes [4,13]. Indeed, the subtractive and additive processes can be successively executed so that the milling tool can reach the surfaces to machine when they are still accessible, while the PAM process can ensure an enhanced freedom of design. Hybrid machines are already commercialized, but they are all relying on AM processes which directly produce a fully dense part as Selective Laser Sintering (SLS) or Direct Energy Deposition (DED) [4,13]. As a result, the machining is carried out in fully dense state and leads to higher cutting stresses, wear of the tool and lower material removal rates, making this technology expensive. Developing a machine able to obtain green parts and to machine them at the green state is then an elegant solution to reduce costs, while ensuring new design possibilities for difficult materials such as ceramics. However, except for highly used alloys (Ti6Al4V, *e.g.*), only few data are available for the machining of additively manufactured materials [12].

Goal and motivation of the study. This study aims to determine if the build or in-plane directions within a zirconia green part obtained by the PAM process can have a non-negligible influence on the cutting forces and surface topography generated during finishing operation performed with milling.

Material and Method

Part geometry and printing. The geometry of the part consists of a cube (side of 20 mm) on top of a cylinder (diameter of 15 mm and height of 15 mm). Both are linked using a 3 mm fillet radius. The milling operations are performed on the cube while the cylinder surface is used for the part fixture. Fig. 1 gives the geometry of the part as well as the reference frame (located at one of the part top corners) which was used for the experiments and the build direction selected for the part printing. The X and Y axes are aligned with two horizontal edges of the cube, while the Z axis is aligned with a vertical edge (Z axis is the inverse of the build direction as shown in Fig. 1).

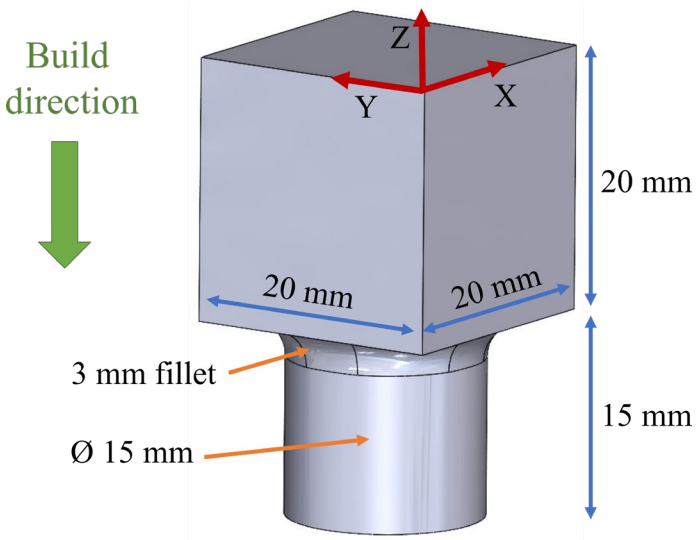

Fig. 1. Part geometry and reference frame.

The part was printed using a Pollen AM Series MC PAM printer by setting the build direction across the part Z axis (see Fig. 1). K2015 pellets from Inmatec were used as feedstock. They are composed of 15wt% polyamide and 85wt% zirconium oxide. The cube is first printed, followed by the cylinder to avoid the need of support structure. The nozzle diameter and layer thickness selected were of 1 mm and 0.35 mm, respectively. These parameters allowed to have a printing time of 25 minutes for the part.

Part machining. A three-jaw chuck was used to clamp the part and the milling operations were conducted with a Stäubli TX200 fitted with a Teknomotor ATC71 electrospindle (maximal power and speed of 7.8 kW and 24000 rpm, respectively). The milling tool used for the operation is supplied by Hoffmann (reference 209425-6, 6 mm diameter, 3 teeth, maximal depth of cut of 19 mm). The cutting conditions were chosen to comply with finishing operations of AM parts. As a result, the axial depth of cut (a_p) was set at 3 mm while the radial depth of cut (a_e) chosen was 0.5 mm. According to a preliminary study, the cutting speed and feed rate were of 339 m/min and 1458 mm/min, respectively.

As depicted in Fig. 2, the part was divided into six zones (each of 3 mm thick) across the build direction (Z axis) and six other zones (each of 3 mm wide) across its in-plane direction (Y axis). Each zone of the in-plane direction corresponds to six different passes. All passes were machined along the part X axis. In total, 216 passes were performed totalizing about 3 minutes of cut within the material.

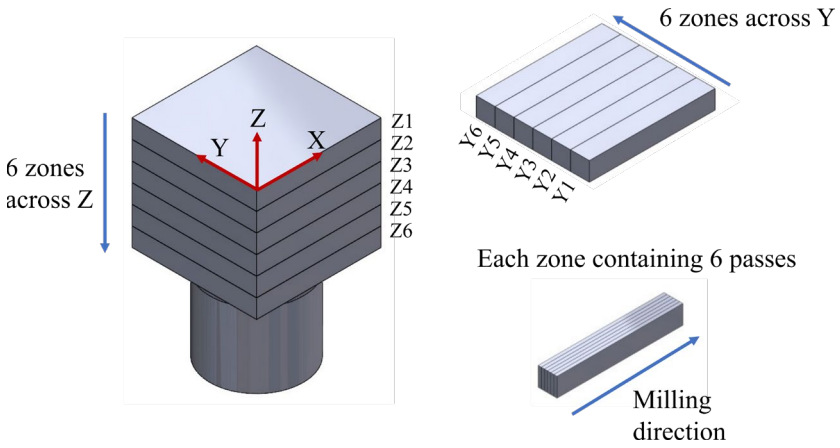

Fig. 2. Zones considered for the milling operations.

Cutting forces and surface topography evaluation. The cutting forces were recorded using a Kistler 9256C2 force sensor coupled with a Kistler charge amplifier 5070A. The DynoWare software executed on a computer as well as a Kistler 5697A2 data acquisition system sampling data at 5 kHz complete the acquisition chain. The reference frame of the cutting sensor is not the same as the frame of the part. Consequently, the total value (Eq. 1) of the X, Y and Z cutting forces components was considered. Fig. 3 gives an example of the total cutting forces signal for three passes of the tests. Finally, the RMS value of the total cutting forces was computed for each pass to have a value representing each pass. These RMS values were then averaged over the six passes contained in each defined zone.

$$F_{tot} = \sqrt{\frac{1}{3} \cdot (F_x^2 + F_y^2 + F_z^2)} \quad (1)$$

Materials Research Proceedings 28 (2023) 1245-1253 https://doi.org/10.21741/9781644902479-135

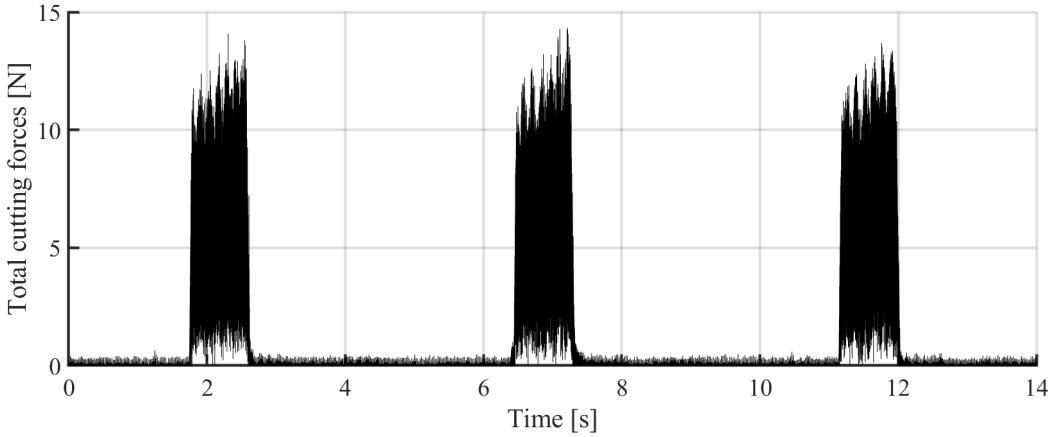

Fig. 3. Example of total cutting forces signal for three passes of the tests.

The surface topography was analyzed qualitatively using a Dino-Lite digital microscope AM7013MZT with DinoCapture software (monitoring of the generation of material pull-out and the existence of porosities inside the parts) and quantitatively with a Diavite DH6 roughness measuring instrument (measurements of Ra and Rt). The evaluation and cut-off lengths (4.8 mm and 0.8 mm, respectively) were selected according to the ISO 4288 standard. The surface topography was evaluated every three passes on the vertical surface generated by side-milling and following the X axis direction.

Results and Discussion

Cutting forces analysis. The cutting forces across the Y and Z zones of the part are depicted in Fig. 4 and 5, respectively. Each graph is given with error bars corresponding to ± σ.

As it can be seen in Fig. 4, the RMS total cutting forces remain stable across the different Y zones with an average of 3.97 N. However, the relative standard deviation ranges between about 29.7% and 38.5%, which is very high. Every bar on the graph represents a total of 6 different tests of 6 passes at different Z heights for a given Y zone. Consequently, the build direction (Z axis) has a non-negligible effect on the cutting forces because of the large standard deviations recorded between the measurement of a given Y zone. Conversely, the in-plane direction (Y axis) does not influence the results since the mean value across the different Y zones is nearly constant.

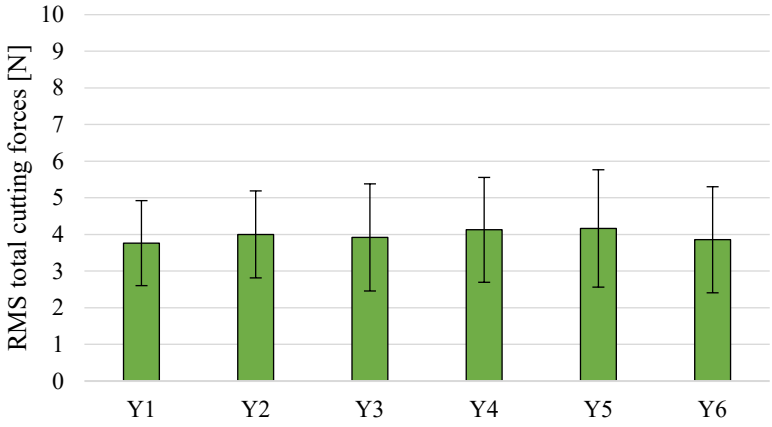

Fig. 4. RMS total cutting forces across the Y zones.

Materials Research Proceedings 28 (2023) 1245-1253 https://doi.org/10.21741/9781644902479-135

The same conclusions can be retrieved from Fig. 5. Indeed, the graph shows a global decreasing trend across the different Z zones. The maximal value is 6.35 N while the minimal value stands at 2.70 N. The cutting forces in the Z6 zone are 57.5% lower than in the Z1 zone.

This confirms the influence of the build direction (Z axis) on the cutting forces. Moreover, it shows that the zones of the part in contact with the build platform of the printer need more force to be cut than those further away. Indeed, Z1 zone corresponds to the first layers deposited on the build platform while Z6 zone is related to the layers near the cylindric part. This difference of cutting forces may originate from the different thermal history applied to the layers in contact with the build platform in comparison with the higher layers. The deposited layers can then exhibit different properties in terms of mechanical properties (micro-hardness, for example). At the knowledge of the authors, no study in literature mentioned this influence for green ceramics parts obtained neither by the PAM process, nor by other AM processes.

Conversely, the average relative standard deviation is stable through all Z zones with values between 9.5% and 13.6%. This confirms that in-plane direction (Y axis) does not influence much the cutting forces. This decreasing tendency is not asymptotical and, since the Z6 zone is near the cylindric part of the part, this change of section and geometry may have an influence on the required cutting forces because of stresses distribution.

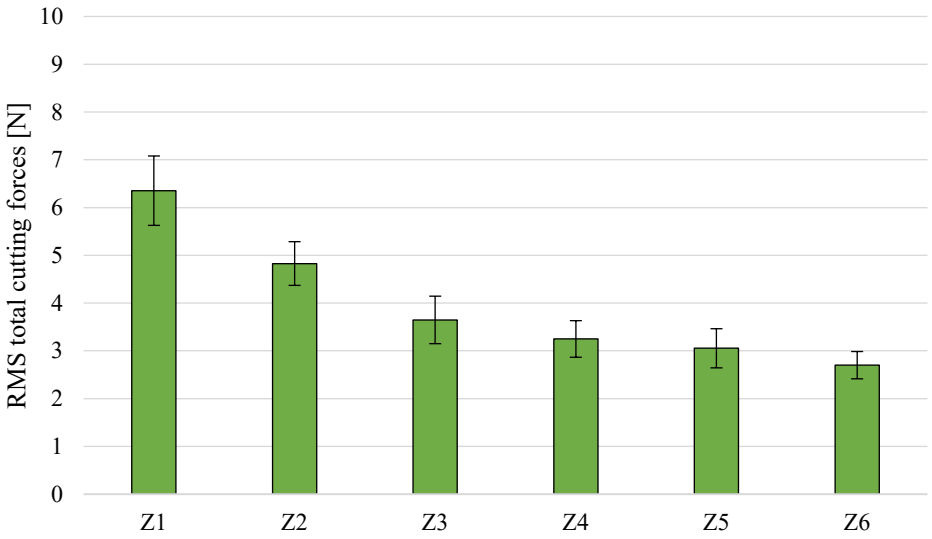

Fig. 5. RMS total cutting across the Z zones.

Surface topography quantitative analysis. Fig. 6 and 7 show the arithmetic roughness evolution across the Y and Z zones of the part. Each graph was given ± σ error bars as well as two red horizontal bars showing the boundaries of the 0.8 µm Ra class, to which the results belong.

As shown in Fig. 6, the Ra results across the Y zones were all within the 0.8 µm Ra class. The values ranged from 0.45 µm to 0.49 µm with a relative standard deviation between 8.5% and 13.4%. Each bar represents the average Ra measured for 6 different tests of 6 passes realized at six different Z positions. Consequently, it shows that neither the in-plane direction (Y axis), nor the build direction (Z axis) significantly influence the arithmetic roughness results.

Materials Research Proceedings 28 (2023) 1245-1253 https://doi.org/10.21741/9781644902479-135

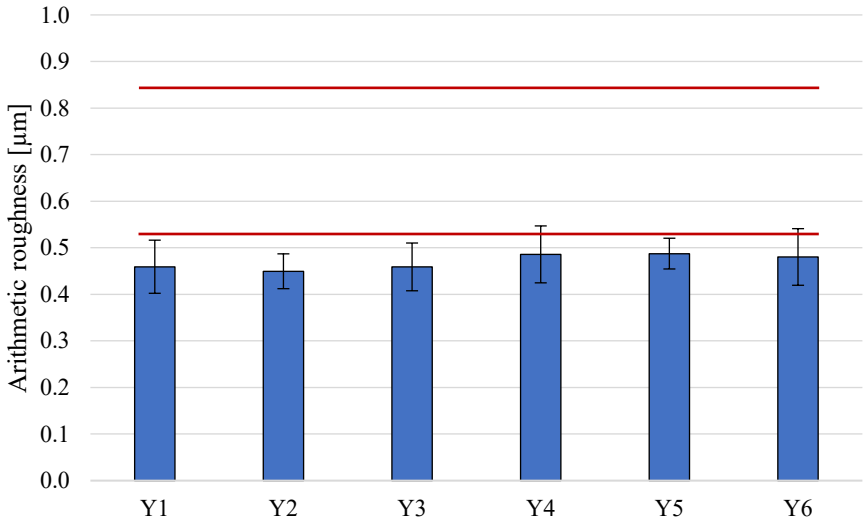

Fig. 6. Arithmetic roughness evolution across the Y zones.

This is also confirmed in Fig. 7 with Ra results across the Z zones between 0.45 µm and 0.49 µm and a relative standard deviation representing from 6.3% to 15.0% of the mean value. This confirms the non-influence of the in-plane and build directions on the arithmetic roughness results. Both graphs also demonstrate the adequacy of cutting parameters to generate a smooth surface topography. Indeed, every pass generates a Ra lower than 1.6 µm with results in the 0.8 µm Ra class. The relatively low standard deviation shows that results are repeatable.

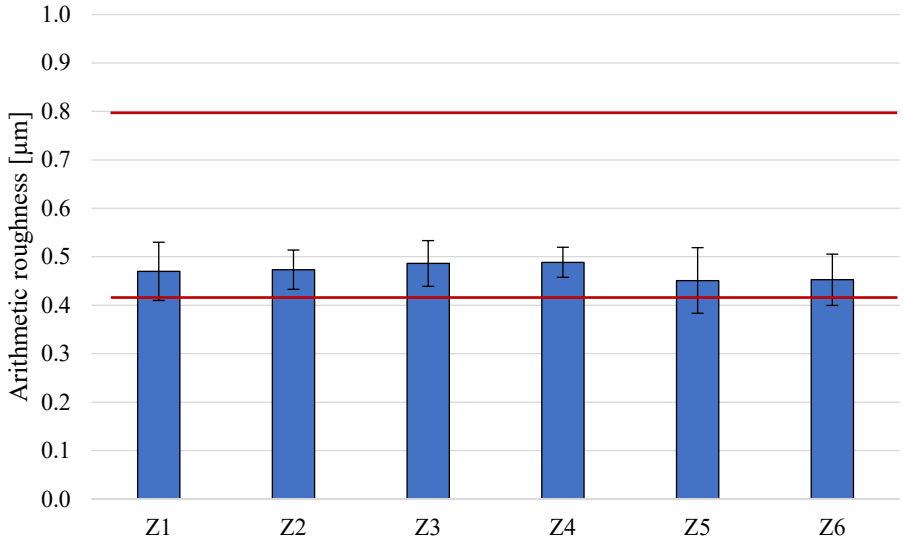

Fig. 7. Arithmetic roughness evolution across the Z zones.

Fig. 8 and 9 give the total roughness measurements obtained across the Y and Z part zones, respectively. Again, each bar of the graph was given a ± σ error bar.

As depicted in Fig. 8, the Rt results across the Y zones were between 2.76 µm and 3.54 µm. The relative standard deviation ranged between 8.6% and 16.6%, except for the Y4 zone where it reached 22.6%. The Y4 zone corresponds to the center of the part and exhibited higher results of Rt compared to the other zones (about 20% higher on average). Some porosities were detected at the center of the part and may influence slightly the Rt measurements.

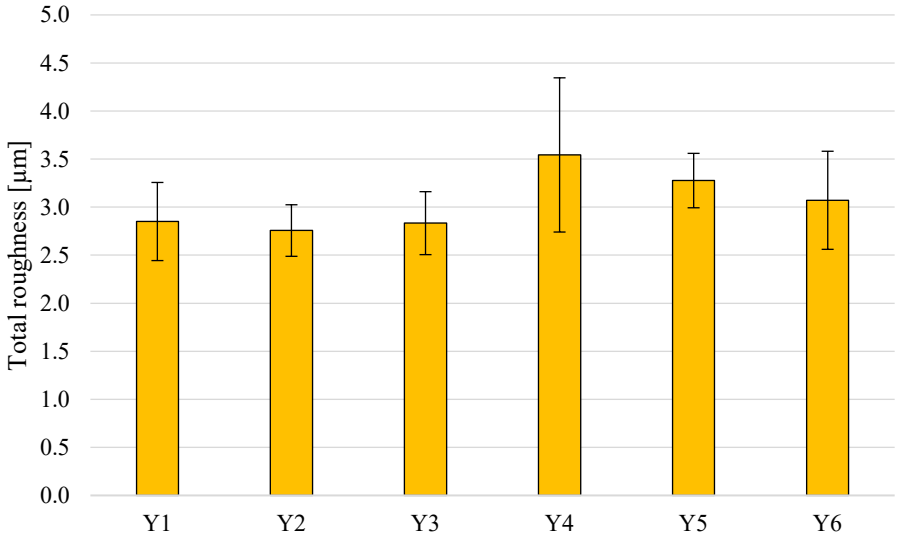

Fig. 8. Total roughness evolution across the Y zones.

By following the build direction (Z axis), the Rt results were between 2.88 µm and 3.30 µm while the relative standard deviation ranged from 7.8% to 19% (see Fig. 9). Even if the mean value varies, all the results are of the same order of magnitude (< 5 µm). Consequently, neither the in-plane nor the build direction (Y axis and Z axis, respectively) influence the total roughness.

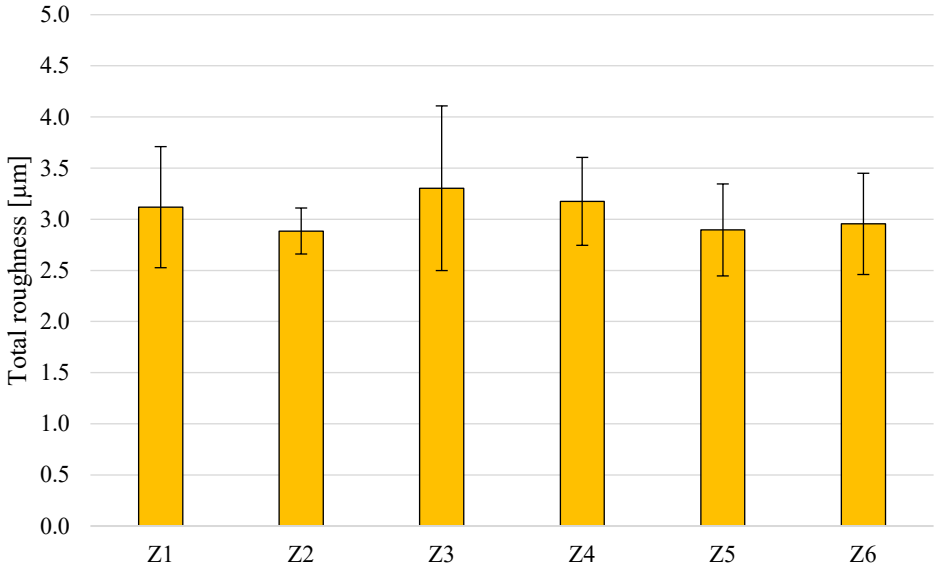

Fig. 9. Total roughness evolution across the Z zones.

Surface topography qualitative analysis. Fig. 10 shows the typical surface topography generated by the milling operation (bottom) compared to the as-built part (top). The bottom part of the picture corresponds to the zones Y1 and Z4. The surface topography obtained after milling is shiny and very smooth.

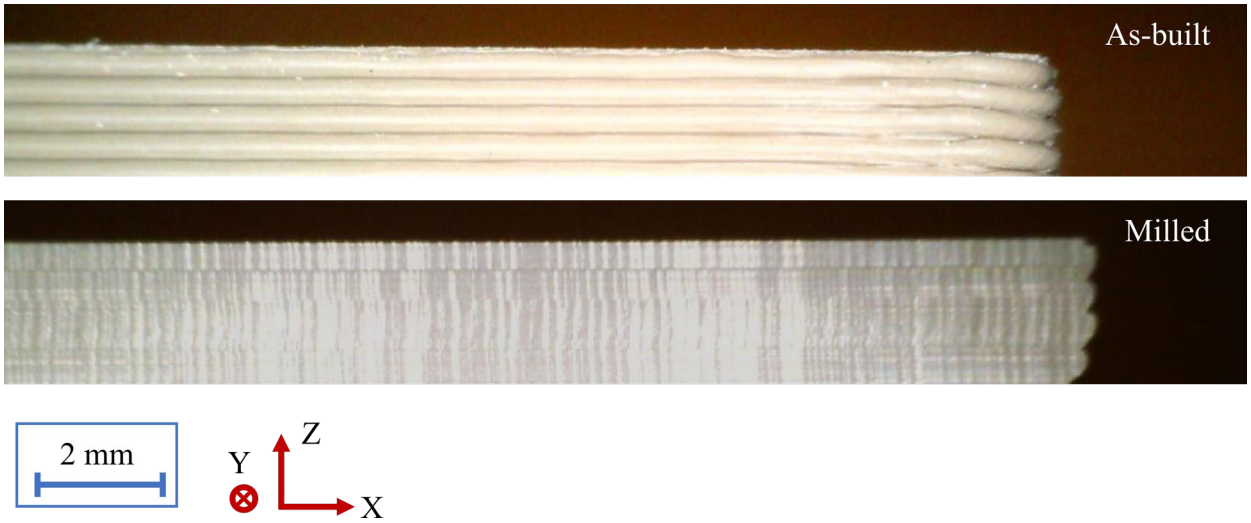

Fig. 10. As-built surface (top) and milled surface of zones Y1 and Z4 (bottom).

Summary

Conclusion. The main findings of this study are:

- The build direction of the part (Z axis) has a significant influence on the cutting forces required to carry out the milling operations. The nearest from the build platform, the higher the cutting forces. When the milling is performed further from the build platform, the cutting forces decrease (up to 57.5% in this study). The experiments do not allow to foresee if this decreasing tendency is asymptotical. The geometry change occurring in Z6 zone (last cubic zone before the transition to the cylindric part) may have an influence on the cutting forces. The in-plane direction (Y axis) does not have a significant influence on the cutting forces.
- From a qualitative point of view, the surface topography generated by the milling operations is smooth and light reflective.
- The arithmetic and total roughness are neither influenced by the build direction (Z axis), nor by the in-plane direction (Y axis) across the part. Indeed, all Ra results belonged to the 0.8 µm Ra class with a maximal relative standard deviation of 15%. So do the Rt results with all values in the same order of magnitude (< 5 µm) with a maximal standard deviation of 22.6%. The center of the part (Y4 zone) exhibited 20% higher Rt results than in the other zones. This may originate from the existence of porosities inside the part.

Perspectives. These are the main perspectives of the work:

- The cutting forces decreasing tendency across the build direction when moving away from the build platform can be further studied. The use of a different part designs with only one geometrical shape (a cube with higher dimensions, *e.g.*) will allow to determine if the cutting forces reach a plateau after a dedicated number of layers deposited. Moreover, micro hardness measurements as well as thermal monitoring can help understanding what physically causes this tendency.
- The influence of the transition between geometrical features (the cube and the cylinder of the part design presented) on the cutting forces can be further investigated by using a different part design.

Acknowledgements
The Wallonian regional government funded this research thanks to a Win²Wal funding instrument (HyProPAM research project, grant number: 2110084). The authors are grateful to the Belgium Ceramic Research Centre (BCRC) for the usage of their Pollen AM Series MC printer and especially to Julien Bossu (UMONS) who printed the part.

References
[1] D. Galusek, K. Ghillányová, Ceramic Oxides, in: R. Riedel, I.-W. Chen (Eds.), Ceramics Science and Technology, Wiley-VCH Verlag GmbH & Co., Weinheim, Germany, 2014, pp. 1-58. https://doi.org/10.1002/9783527631940.ch13
[2] E. Ferraris, J. Vleugels, Y. Guo, D. Bourell, J.P. Kruth, B. Lauwers, Shaping of engineering ceramics by electro, chemical and physical processes, CIRP Ann. 65 (2016) 761-784. https://doi.org/10.1016/j.cirp.2016.06.001
[3] A. Demarbaix, M. Mulliez, E. Rivière-Lorphèvre, L. Spitaels, C. Duterte, N. Preux, F. Petit, F. Ducobu, Green Ceramic Machining: Determination of the Recommended Feed Rate for Y-TZP Milling, J Compos. Sci. 5 (2021) 231. https://doi.org/10.3390/jcs5090231
[4] P. Parenti, S. Cataldo, A. Grigis, M. Covelli, M. Annoni, Implementation of hybrid additive manufacturing based on extrusion of feedstock and milling, Procedia Manuf. 34 (2019) 738-746. https://doi.org/10.1016/j.promfg.2019.06.230
[5] M.K. Thompson, G. Moroni, T. Vaneker, G. Fadel, R.I. Campbell, I. Gibson, A. Bernard, J. Schulz, P. Graf, B. Ahuja, F. Martina, Design for Additive Manufacturing: Trends, opportunities, considerations, and constraints, CIRP Ann. 65 (2016) 737-760. https://doi.org/10.1016/j.cirp.2016.05.004
[6] J. Gonzalez-Gutierrez, S. Cano, S. Schuschnigg, C. Kukla, J. Sapkota, C. Holzer, Additive manufacturing of metallic and ceramic components by the material extrusion of highly-filled polymers: A review and future perspectives, Materials 11 (2018) 840. https://doi.org/10.3390/ma11050840
[7] Smartech Analysis, Ceramics Additive Manufacturing Markets 2017-2028, an opportunity analysis and ten-year market forecast, 2018. https://www.smartechanalysis.com/reports/ceramics-additive-manufacturing-markets-2017-2028/
[8] S.C. Altıparmak, V.A. Yardley, Z. Shi, J. Lin, Extrusion-based additive manufacturing technologies: State of the art and future perspectives, J. Manuf. Processes 83 (2022) 607-636. https://doi.org/10.1016/j.jmapro.2022.09.032
[9] M.A. Krolikowski, M.B. Krawczyk, Does Metal Additive Manufacturing in Industry 4.0 Reinforce the Role of Substractive Machining, in: J. Trojanowska, O. Ciszak, J.M. Machado, I. Pavlenko (Eds.), Advances in Manufacturing II, Springer International Publishing, Cham, 2019, pp. 150-64. https://doi.org/10.1007/978-3-030-18715-6_13
[10] B.N. Turner, S.A. Gold, A review of melt extrusion additive manufacturing processes: II. Materials, dimensional accuracy, and surface roughness, Rapid Prototyp. J. 21 (2015) 250-261. https://doi.org/10.1108/RPJ-02-2013-0017
[11] W. Hung, Post-Processing of Additively Manufactured Metal Parts, in: D.L. Bourell, W. Frazier, H. Kuhn, M. Seifi (Eds.), Additive Manufacturing Processes, ASM International, 2020, pp. 298-315 https://doi.org/10.31399/asm.hb.v24.a0006570
[12] N. Uçak, A. Çiçek, K. Aslantas, Machinability of 3D printed metallic materials fabricated by selective laser melting and electron beam melting: A review, J. Manuf. Process. 80 (2022) 414-457. https://doi.org/10.1016/j.jmapro.2022.06.023
[13] J.M. Flynn, A. Shokrani, S.T. Newman, V. Dhokia, Hybrid additive and subtractive machine tools - Research and industrial developments, Int. J. Mach. Tool. Manuf. 101 (2016) 79-101. https://doi.org/10.1016/j.ijmachtools.2015.11.007